JOURNAL OF KUFA–PHYSICS
www.uokufa.edu.iq/journals/index.php/jkp | ISSN: 2077–5830

A new approach to prepare nano hydroxyapatite from oyster shells used for dental applications

Kifayah K. Thbayh[1]* **Rafid M. AlBadr[2]** **Kareema M. Ziadan[1]**

[1] Department of Physics, College of science, University of Basrah, Basrah, Iraq.

[2] College of Dentistry, University of Basrah, Basrah, Iraq .

*Corresponding Author E-mail: kifayahkarad18@gmail.com

ARTICLE INF

Article history:
Received: 27 AUG, 2022
Revised: 02 OCT, 2022
Accepted: 07 OCT, 2022
Available Online: 17 DEC, 2021

Keywords:

Nano hydroxyapatite
XRD
Oyster shells
FTIR
SEM

ABSTRACT

HA (hydroxyapatite) is considered one of the biomaterials widely, it is applied in many applications like the medical and dentistry. In this research, NHA powder was prepared from some natural source rich in calcium carbonate, it was prepared by calcination method at 1200 ℃ for 2 hours. The samples were diagnosed by using various diagnostic tests including scanning electron microscopy (SEM), X-ray diffraction (XRD), Fourier transform infrared (FTIR), X-ray spectroscopy (EDX), and the density measurements. The XRD results showed that HA as-prepared high purity and the crystallite size as around 63.561± 11.327 nm, while the particle sizes≈ 63 nm according to BET, also EDX clearly showed elements (Ca, P, O). As for the density of NHA, it was measured and found to be equal to (2.98±0.1) g/cm^3. Characterization results (XRD, SEM, EDX, FTIR, and BET) showed that the morphological and structural properties of the Hydroxyapatite.

DOI: http://dx.doi.org/10.31257/2018/JKP/2022/140205

طريقة جديدة لتحضير نانو هيدروكسيباتيت من قشور المحار المستخدمة في تطبيقات طب الأسنان

كفاية كراد ذبيح[١] **رافد مصطفى البدر[٢]** **كريمة مجيد زيدان[١]**

[١] قسم الفيزياء، كلية العلوم، جامعة البصرة، البصرة، العراق.
[٢] كلية طب الأسنان، جامعة البصرة، البصرة، العراق.

الـــخُـــلاصـــة

يعتبر هيدروكسيباتيت من المواد الحيوية المستخدمة على نطاق واسع في الطب وطب الأسنان. في هذا البحث تم تحضير مسحوق NHA من بعض المصادر الطبيعية الغنية بكربونات الكالسيوم، وتم تحضيره بطريقة التكليس عند درجة حرارة تساوي ١٢٠٠ ℃ لمدة ساعتين. تم تشخيص العينات باستخدام اختبارات تشخيصية مختلفة، مثل الفحص المجهري الإلكتروني (SEM)، حيود الأشعة السينية (XRD)، مطافيه الاشعة تحت الحمراء (FTIR)،

الكلمات المفتاحية:

نانو هيدروكسيباتيت
XRD
اصداف المحار
FTIR
SEM

التحليل الطيفي للأشعة السينية (EDX)، وكذلك قياسات الكثافة. أظهرت نتائج XRD أن HA محضرة بدرجة نقاءه عالية وحجم بلوري حوالي ٦٣.٥٦١ ± ١١.٣٢٧ نـانومتر، بينمـا أحجـام الجسيمات ٦٣ نـانومتر وفقًا لـ BET، كمـا أظهرت EDX بوجود العناصـر التاليـة (P, Ca, O). اما بالنسبة لكثافة NHA تم قياسها ووجد أنهـا تسـاوي (٢.٩٨ ± ٠.١) غم/سم^{٣}. القياسـات التاليـة (XRD، SEM،EDX ، FTIR ،BET) وضـحت كـل الخصـائص المورفولوجيـا والهيكلية لمادة لهيدروكسيباتيت.

1. INTRODUCTION

Repairing damaged bones due to chronic diseases and various traumas is a challenge for clinicians and because this requires a biological structure similar to that of bone. Hydroxyapatite (HA) (Ca_{10} (PO_4) $_6$ $(OH)_2$ is a calcium phosphate ceramic that belongs for the apatite family of calcium phosphates and is a biologically active ceramic [1]. Bio ceramics have good mechanical properties and appropriate for load bearing applications PO_4 [2]. And excellent biocompatible in orthopedic application. It is capable of fusing with bone without triggering any local toxicity and inflammation [3]. Hydroxyapatite is the main vital mineral component found in human hard tissues, and bone structure contains about 65 wt. %, also enamel consisting of more than 60% by weight [4,5]. Because of its biocompatibility and capability to form bone, it has been extensively studied for medical and dental application and also it can be used in several ways like Implant coating, orthopedic scaffold, orthotics filling or drug delivery systems [1], but its use in dentistry is constantly increasing. Recent studies have also demonstrated the value and requirement of biomimetic oral health products using nano-sized hydroxyapatite particles in contemporary preventive dentistry [6, 7].

Oyster shells are one of the available ready-mades and low-cost natural waste, which mainly consists of calcium carbonate (98%) with very negligible impurities (trace elements such as In recent years though, there have been several techniques of synthesis of Nano Hydroxyapatite (NHA) which have been successful to precise control structure and size of NHA particles. Mg, Sr, K and Na) [8]. Also Oyster shells can be attractive features for converting biological material due to its chemical composition into hydroxyapatite (HA) powders.

In recent years though, there have been several methods of synthesis of Hydroxyapatite (NHA) which have been successful. For the production of synthetic HA and through precise control of its structure, several methods are It has been described in the literature. Szcze´s et al. [5]. Methods for preparing HA were classified to five groups: (1) dry methods (solid-state, mechanical mechanical methods) [9]. (2) Wet methods (chemical precipitation, hydrolysis, gel solution, hydrothermal, emulsion or sonochemical) [10]. (3) High temperature processes (combustion, pyrolysis method) [11]. (4) Synthesis based on bio-sources [12]. (5) collection methods (eg hydrothermal - micro-emulsion, hydrothermal - mechanical, hydrothermal - hydrolysis, etc.) [13] (Figure 1).

The co- Precipitation method is one of the most successful and most common techniques due to its simplicity, quick preparation as well as ease of control of particle size, shape and structure, farther more, various possibilities to modify the overall homogeneity of the product [14]. It has been used in the preparation of many nanoparticals such as CaF_2, TiO_2, ZnO and Fe_3O_4 [15,16].

In recent years, although there are many methods of hydroxyapatite synthesis, the methods of preparing it with certain properties

are still a challenge for the possibility of forming toxic intermediate products during synthesis [11].

The importance of these materials has prompted researchers to develop innovative nanoparticles for various applications. Nanomaterials technology has been widely used in medical applications (in dental materials) in order to increase their efficiency from a physical and mechanical point of view, such as in composites, cements and ceramics. This is due to the properties possessed by nanomaterials, their small size, ease of formation and other important properties. Therefore, there was wide interest by scientists to develop Nano-apatite because it is a biological material similar in its Be similar to the mineral component of bone. It has been used extensively in many medical applications as a filler to replace damaged bones, as well as in various applications such as dental and maxillofacial applications. In recent years though, there are many hydroxyapatite synthesis methods, [11]. Much effort has been made to synthesize NHA from abundantly materials available natural sources in the environment, such as the mammalian sources. Water or the marine sources, Sources of psoriasis, Plant sources and algae, and Mineral sources [2, 17-20]. In addition, Physical properties such as the degree of thermal equilibrium and purity, its Particle shape and size, all these are important qualities for the purity and high quality of each form for use in biomedical applications [21, 22].

In this paper, Nano-hydroxyapatite (NHA) was prepared from oyster shells. It is considered the main natural source of hydroxyapatite. Oyster shells are biological waste whose main component is calcium carbonate that makes up 96%, as well as Other trace elements such as Na, Mg, K, and Sr. It is a raw material for the manufacture of hydrochloric acid [8], and it is usually available on the banks of rivers in abundance and at low prices. The shells represent 55% of mussels. The shells of oysters (fossils) were collected and placed in distilled water for 24 hours, then dried and peeled to remove dirt residues [23].

1. Experimental

2.1 materials

Thirty oyster shells from the Faw city were collected. The oyster which were measured (3 cm to 5 cm in length) were thoroughly purify from impurities then washed with water and alcohol several times (figure 1). The oyster shell has been dries through using oven at 80°C for a period of 24 hours following washing. The oyster shells were crushed by using a pestle and ground, then sieved with a sieve below than 36 µm were obtained using an auto sieve shaker (Mates, A060-01, Germany) approximately 75 g obtain of CaCo3 from oyster shells. To transform $CaCO_3$ into calcium oxide CaO. The powder ($CaCO_3$) was placed in electrical furnacea (MV MIHM-VOGT P6/B) and then burned to 1200 ℃ for 2 hr at a rate increase 10^0 C/min. Then the crop is cooled and ground again and sieved using a 500-mesh sieve to obtain calcium oxide particles below than < 25 µm.

2.2. Synthesis of NHA

Co-precipitation method to synthesis NHA nanocrystals (NHA powders have been prepared at room temperature with buffer pH 10), 1 mol CaO (obtained from oyster shell) was a dissolved in 100 ml distilled water taken in 500 ml conical flask. 0.6 mol H_2PO_4 was added into the flask under vigorous stirring on a magnetic stirrer. The mixed solution was stirred for 2 h to transform the transparent reaction mixture into opaque white suspension gradually. Then, the mixture was centrifuged for 10 min at 5000 rpm and washed three times with distilled water via centrifugation to remove the residual calcium and the PO_4 ions. Finally, the solid product has been kept in an oven at 120 ◦C for 48 hours as show in (***Figure 1***)

$$Ca_2CO_3 \rightarrow CaO + C0_2$$

$$CaO + H_2O \rightarrow Ca(OH)_2$$

$$10Ca(OH)_2 + 6H_3PO_4 \rightarrow Ca_{10}(PO4)6(OH)2 + 18H_2O$$

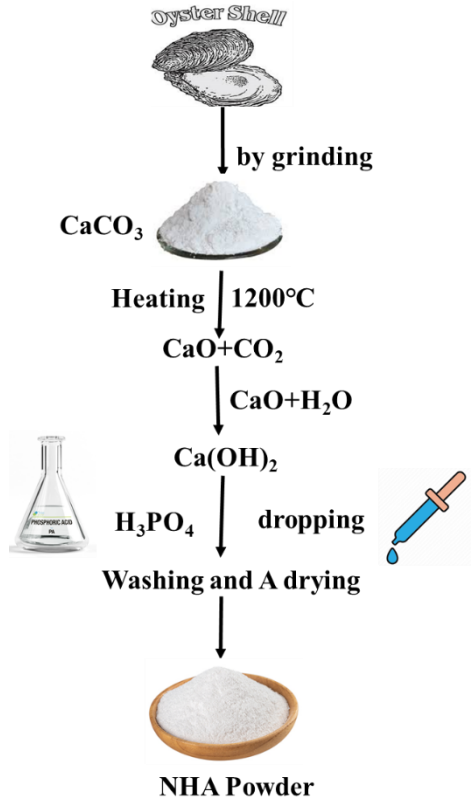

Figure 1: Synthesis route for producing NHA powder from oyster shells

2.3. Characterization of NHA

X-ray diffraction (XRD) was performed of oyster shell, CaO and syntheses NHA. XRD patterns used the Cu KD = 1.5405 A° radiation (Philips PW 1700 series diffract meter, Leiden, Netherlands) scanned between 2θ (10 - 70◦) with a step size of 2θ = 0.02◦ in continuous mode and a count time of 0.35 Sec per step. The crystallite size (D) of the glass samples was determined by using Scherer equation.

$$D = \frac{\beta\,\lambda}{W\cos\theta} \quad \ldots\ldots (1)$$

where λ represents the incident X-ray wavelength (0.154060 nm), β Scherer A constant between 0.85 -0.99 This depends on the particle morphology (β = 0.89) for spherical crystals with cubic symmetry), θ represents the diffraction angle, and W is the full width at half maximum (FWHM in radians). The diameter of the sphere (L) can be estimated [24]:

$$< L > = \frac{4}{3} D \quad \ldots\ldots\ldots (2)$$

Where D crystallite size.

Also XRD was used to determine the crystal size of NHA along the orbit of the c axis and the a axis by applying lattice planes spacing can be expressed as follows.

$$d = \frac{a_\circ}{\sqrt{h^2 + k^2 + l^2}} \quad \ldots\ldots\ldots (3)$$

a_0: lattice constant, here h, k, l are the miller indexes of the set lattice planes under consideration, we can write the quadratic form

$$\sin^2\theta = \frac{\lambda}{2a_0}^2 ((nh)^2 + (nk)^2 + (nl)^2) \quad \ldots\ldots\ldots (4)$$

To characterize the morphology and size, scanning electron microscopy (SEM) was used. NHA and size particles. (VEGA TESCAN - Czech). As for the calcium oxide picture, it shows a significant difference from the shells of oysters, and this indicates the process of releasing carbon dioxide during the calcination process. Microscope images reveal the outer distances of the sample[25]. In addition, X-ray analyser (EDX), associated with SEM, and It was used for semi-quantitative verification of chemical compositions. The density of the substance was measured using a specific gravity bottle (density bottle). Where the weight of the bottle was measured when it was empty without any additives (W_{pyc}) [26].

$$P_{Pow} = \frac{Wpow}{W_{pyc-wat} - (W_{pyc-wat-pow} - Wpow)} \quad \ldots\ldots (5)$$

Transform infrared (FTIR; Nicolet Magna-IR 550) uses Fourier analysis spectrophotometer, Madison, WI) was used to analyse the functional groups of oyster shells (CaCO3), CaO, commercial HA and NHA prepared from oyster shells. FT-IR spectra were acquired over the 500-4000 cm-1 region using the KBr pellet technique. The specific surface

area of oyster shell powder was calculated by Brunauer-Emmett-Teller (BET) analysis. The BET method was also used in conjunction with Chembet-3000 QUANTACHROME. The mean diameter (dBET) obtained by applying the BET method is represented as:

$$d_{BET} = \frac{6}{A_s \rho} \ldots\ldots\ldots (6)$$

Whereas is the specific surface area (m^2/g) and ρ is the theoretical density of the hydroxyapatite 3.18 g/Cm^3. Malvern Zetasizer version 7.03 (serial number: MAL1032006) particle size analyser was used to analyse The particle size that is sintered compound NHA powder. The volume distribution report was calculated by intensity and the statistical report volume by severity.

1. Result and Discussion

In order for us to obtain biomaterials with nanostructure Advantages restorative dental material, a great deal of interest has been revealed to NHA with natural waste. The XRD pattern of oyster shells (Figure 2) shows characteristic peaks at the 2θ (26.17, 27.16, 29.36, 33.12 and 45.87), which are fitting with identified JCPDS (CaCO3) the file No. 085-1108. The result did not show any extraneous phases corresponding to CaCO3 suggesting that CaCo3 with high purity. In addition, the XRD Pattern were used to calculated the crystalline size D (nm) from equ.1 for oyster shells indicate to 34.592± 10.086 nm. Figure 3 Illustrates that the XRD spectra from calcium oxide CaO, from which we were observe three distinct peaks at 2θ (32.1261, 37.2826 and 53.77) and several small peaks, appeared to the crystalline nature of the CaO, also, the crystalline sizes of CaO was calculated and indicate to 63.373±11.17 nm.

Figure 4 shown the XRD pattern of NHA contain many sharp peaks appeared which mean HA have high crystallinity, furthermore, XRD pattern obtain with d-spacing values of 4.920 Å, 3.04 Å and 2. 79 Å and the d spacing value also exactly matches hexagona dipyramidal phase. From Table 1 Influence of the lattice parameters, the HA hexagonal-dipyramidal phase axis= axis and c axis were calculated as well as crystallite sizes (D) from the corresponding X-ray diffract grams' fig 3. The parameters values of NHA were near to the JCPDS standard (an axis= b axis =9.418^0 A and c axis=6.884 ^{0} A) but have slight differences among them. These slight differences in the calculation of crystallographic parameters can be due to the purity of NHA, which depends on the reaction components and preparation methodology (63.55 nm).

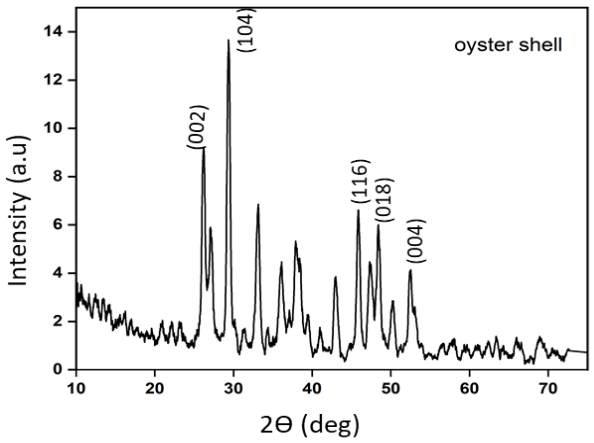

Figure 2: Shows XRD for Oyster shell powder ($CaCO_3$)

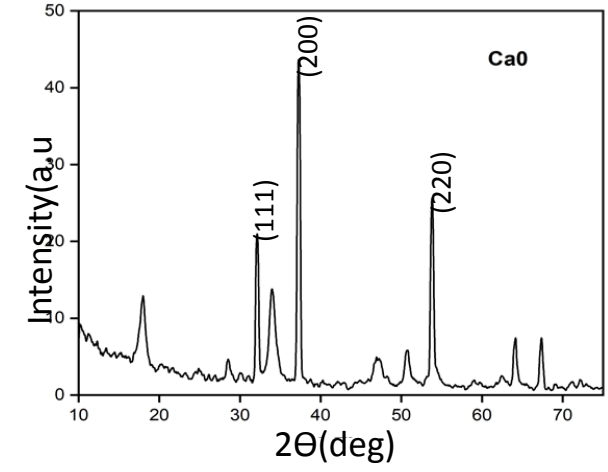

Figure 3: shows XRD for CaO powder

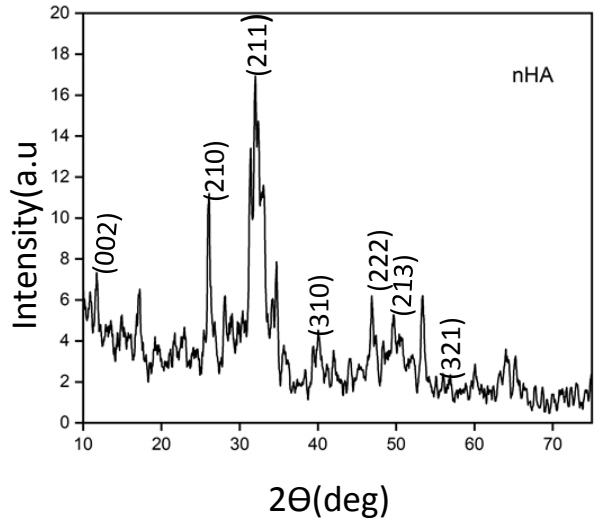

Figure 4: shows XRD for NHA powders.

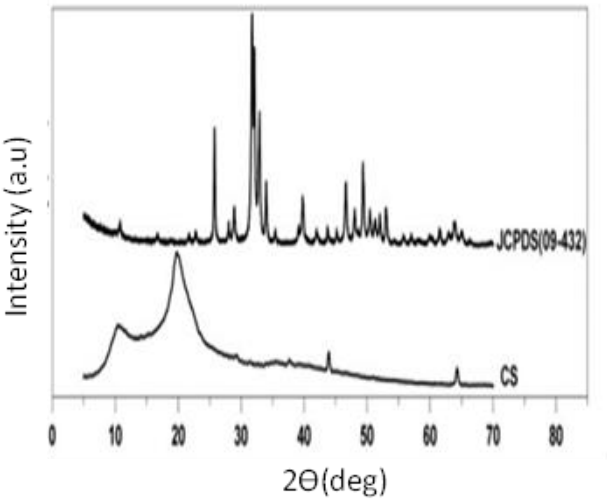

Figure 5: shows XRD for the NHA powder (standard) as reference.

Table 1. The particle size analyses of a HANPs.

2θ Degree	Miller index (hkl)	d value (Å)	Crystalline size D (nm)	Dimeter <L> (nm)	lattice constant a_0 (Å)
18.0273	002	4.92	67.35	89.80	9.49
28.6346	202	3.55	68.65	91.53	9.47
29.3679	210	3.04	41.26	55.02	6.8
34.0558	211	2.63	69.56	92.75	6.44
47.0902	222	1.92	70.08	116.11	6.68
50.7485	213	1.79	55.24	73.65	6.73
54.3093	321	1.68	72.76	99.68	6.32

Generally, crystallization is influenced by physical conditions such as temperature, pH, ionic strength and presence of different additives[27,28] .

This crystallographic structure is more similar to natural bone mineral. This further confirms the XRD findings that the NHA is completely transformed to CPP. A similar observation was reported by Gomze-Morales et al.

Morphological results from SEM images show images of NHA, where we see in the ***Figure 6*** that NHA contains fine lumps and has a surface shape similar to commercial NHA. It also contains a porous and interconnected morphology. This supports its use in medical applications, especially bone tissue[29].

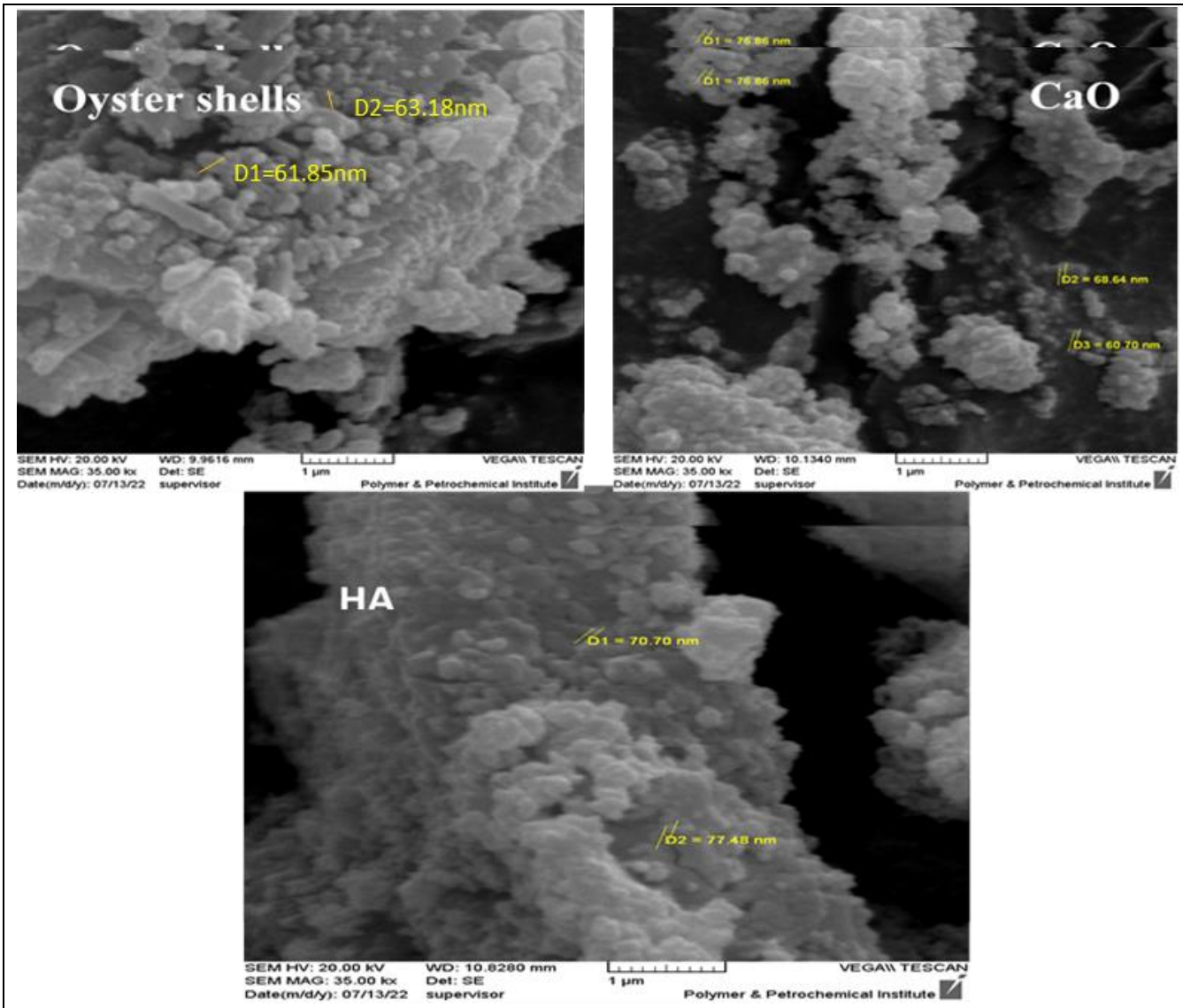

Figure 6: (a) SEM images of Oyster shells, (b) CaO and (c) NHA

The pore size ranges from 0.3 to 1µm, which may be an advantage for the circulation of the physiological fluid when it is used for biomedical purposes.

EDX detected the emission of elements of carbon (C), oxygen (O), and chlorine (Cl). The percentage (wt%) of all elements before SDS adsorption was investigated as following order: C (62.30%) > O (37.07%) > Cl (0.63%). Similarly, the percentage (wt.%) of all elements present in Pinus densiflora cone after adsorption was investigated as following order: C (62.24%) > O (37.65%) > Cl (0.10%). As shown in, EDX detected the As shown in ***Figure 7***, EDX detected for the Oyster shells the result shown that Oyster shells consist of a high percentage of calcium carbonate, approximately 96% and 4 % of some organic element[20]. shows the chemical composition of pure oyster shells powder as it consists of elements (CaO, O, C) [28]. Figure 8, shown the chemical composition of CaO prepared from burning oyster shells, EDX detected that CaO consists of elements Ca, O denoted ~ 47, 53% respectively.

As for NHA powder prepared from the reaction of $Ca(0H)_2$ with H_3PO_4, its chemical composition is shown in the ***figure 9*** and it consists of the elements (Ca, P, O*)* [30].

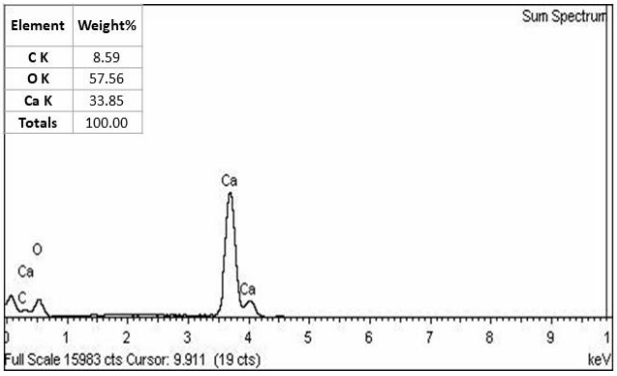

Figure 7: EDX images of Oyster shells

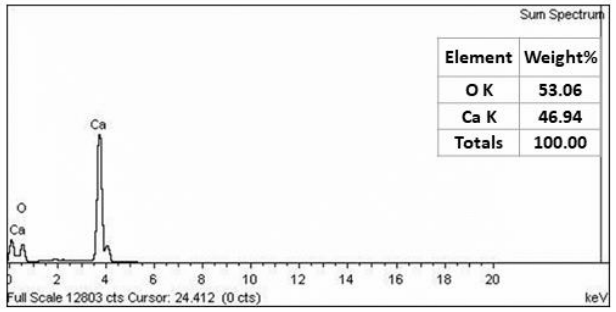

Figure 8: EDX **images of CaO**

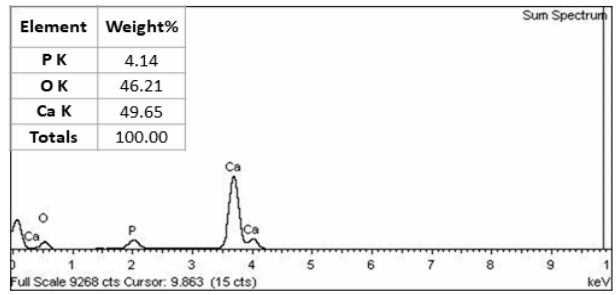

Figure 9: EDX images of NHA

The result density is (2.98±0.1), which is similar to[31]. Transform infrared (FTIR; Nicolet Magna-IR 550) Fourier analysis was used spectrophotometer, Madison, WI) is used to analyse the functional groups of oyster shells (CaCO3), CaO, commercial HA and NHA prepared from oyster shells. FT-IR spectra were acquired over the 500-4000 cm-1 region using the KBr pellet method Figure 10 show us the FTIR spectroscopy for oyster shells, CaO and NHA. Through spectroscopic analysis of oyster shell powder, we note that it consists of four basic bands, which can be described by the vibrational patterns of aragonite and represent the crystalline form of $CaCO_3$ [32].

From the Figure, we note the effective bonds represented by $CaCO_3$, which appears in (712-860 cm^{-1}), while we observe it in CO_3 at (1082 cm^{-1}), as well as the C-O bond that we see in (1477 cm^{-1}) [21]. In addition, by analysing (FTIR) CaO of powder, the formed functional groups represented by CO, O-H and CaO were known. We note from Figure (9) the functional group of oyster shells calcined at a temperature of 1200 ℃ we see it between 426-458 cm^{-1}, as well as O-H we see it in 2435-2643 cm^{-1} as shown in Table 2 [33].

Most of the characteristic chemical bonds of NHA are represented by phosphate, carbonate and hydroxyl [34,35]. The (FTIR) demonstrated the nanocrystalline structure of NHA, from Figure (9) we observe the bands at 470 consistent with the vibrational reactions of (ν4 PO4-3). As for the bands 565-603 cm^{-1}, which are consistent with the vibrational modes (ν4 PO4-3), the CO was observed to be between 1420 cm^{-1} (ν3, asymmetric expansion) and 872 (ν2, outside the plane curve) where it represents the formation of carbonate apatite, which is the reaction resulting from the absorption of carbon dioxide by the atmosphere during the process of apatite synthesis [34].

The broadband in the region of 3000-3600 cm-1 is attributed to water absorption. Thus, these FTIR results are those of successful NHA and the like. For oyster shell powders, calcium oxide, and NHA, the detected Functional groups and their corresponding functions displayed in Table 2.

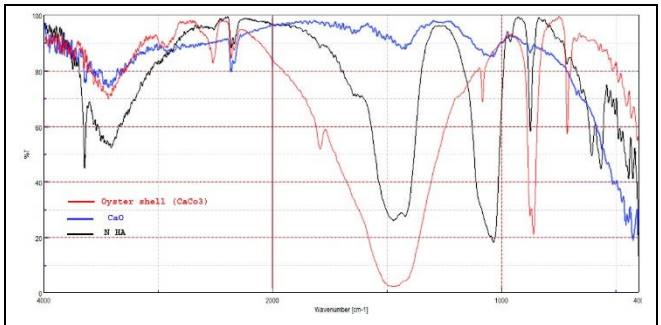

Figure 10: presented FTIR spectra of oyster shells ($CaCO_3$), CaO, and NHA

Table 2: Represents the effective bonding sites for oyster shells, CaO, and NHA.

	Wave number (cm^{-1})	Functional group
Oyster shells (CaCO3)[32]	712	$CaCo_3$ (γ4 mode) aragonite
	860	CaCo3 (γ2 mode)
	1082	(γ1 mode) the symmetric stretching of CO3 appears in the aragonite spectra.
	1477	Inappropriate expansion of the carbonate ion (v3) (calcite), (aragonite)C-O bond
	1788	Inappropriate expansion of the carbonate ion (v1 + 4) (calcite)
	3437	hydroxy group (O-H stretching)
CaO	426	Ca-O bond
	458	Ca-O bond
	1421	o v2 symmetric and v3 asymmetric stretching of CO3 group of the calcite
	2435	hydroxy group (O-H stretching)
	2643	hydroxy group (O-H stretching)
	470	v2 Asymmetric bending vibration PO4 3
	565	v4 Asymmetric bending vibration PO4 3-
	603	v4 Asymmetric bending vibration PO4 3-
	872	v2 Asymmetric bending vibration CO3
	1042	v3 Asymmetric bending vibration PO4 3-
	1420	o v2 symmetric and v3 asymmetric stretching of CO3 group of the calcite
	2364	hydroxy group (O-H stretching)
	2426	hydroxy group (O-H stretching)
	2644	hydroxy group (O-H stretching)
	3747	hydroxy group (O-H stretching)
NHA	470	v2 Asymmetric bending vibration PO4 3
	565	v4 Asymmetric bending vibration PO4 3-
	603	v4 Asymmetric bending vibration PO4 3-
	872	v2 Asymmetric bending vibration CO3
	1042	v3 Asymmetric bending vibration PO4 3-
	1420	o v2 symmetric and v3 asymmetric stretching of CO3 group of the calcite
	2364	hydroxy group (O-H stretching)
	2426	hydroxy group (O-H stretching)
	2644	hydroxy group (O-H stretching)
	3747	hydroxy group (O-H stretching)

To estimate particles specific surface area of NHA, Brunauer-Emmett-Teller (BET) analysis was performed. BET measurements of NHA effectively found a specific surface area of 4.96 m^2g^{-1}. This, thus, corresponded to the size particles of NHA is ≈ 63 nm according to equ.1. Finally, the density of NHA calculated from equ. 5 which denoted 2.98±0.138 g/cm^3 was the nearly as that theoretical density 3.18 g/cm^3. Consequently, the best condition for hydroxyapatite synthesis was seen to be from oyster shell powders.

4. Conclusions

This study is devoted to synthesizing NHA particles from oyster shell powders. The calcinations process of the original oyster shell at the temperatures of 1200ºC for two hours was the most complete transformation from $CaCO_3$ to CaO. The prepared NHA powders at different pH and the results have been shown that, at pH 10 the crystallinity was improved. Although the oyster shell is a waste material, the present investigation shows that the NHA nanocrystalline can be successfully prepared by a simple precipitation method at room temperature from the oyster shell. The particle size of the Nano hydroxyapatite was 60 nm. Moreover, the characteristics of synthesized HA were quite comparable to those prepared from the other methods of homogeneous NHA for subsequent usage in biomedical and orthopedic applications.

5. REFERENCES

[1] R. Murugan, F. Yazid, N. S. Nasruddin, and N. N. M. Anuar, "Effects of nanohydroxyapatite incorporation into glass ionomer cement (GIC)," Minerals, vol. 12, no. 1, pp. 1–10, 2022, doi: 10.3390/min12010009.

[2] Sawittree Rujitanapanicha, Pitoon Kumpapanb, Panthong Wanjanoi" Synthesis of Hydroxyapatite from Oyster Shell via Precipitation" 1876-6102 © 2014 Elsevier Ltd. This is an open access article under the CC BY-NC-ND license

[3] M. K. Herliansyah, D. A. Nasution, M. Hamdi, A. Ide-Ektessabi, M. W. Wildan, and A. E. Tontowi, "Preparation and characterization of natural hydroxyapatite: A comparative study of bovine bone hydroxyapatite and hydroxyapatite from calcite," Mater. Sci. Forum, vol. 561–565, no. PART 2, pp. 1441–1444, 2007, doi: 10.4028/0-87849-462-6.1441.

[4] "Influence of hydrothermal synthesis parameters on the properties of hydroxyapatite nanoparticles" Sylwia Kuśnieruk*§, Jacek Wojnarowicz, Agnieszka Chodara, Tadeusz Chudoba, Stanislaw Gierlotka and Witold Lojkowsk-Beilstein J. Nanotechnol. 2016, 7, 1586–1601. https://doi.org/10.3762/bjnano.7.153
Received 18 Apr 2016, Accepted 13 Oct 2016, Published 04 Nov 2016

[5] W. Suchanek and M. Yoshimura, "Processing and properties of hydroxyapatite-based biomaterials for use as hard tissue replacement implants," Journal of Materials Research, vol. 13, no. 1. pp. 94–117, 1998, doi: 10.1557/JMR.1998.0015.

[6] L. Li et al., "Repair of enamel by using hydroxyapatite nanoparticles as the building blocks," J. Mater. Chem., vol. 18, no. 34, pp. 4079–4084, 2008, doi: 10.1039/b806090h.

[7] N. Roveri et al., "Surface enamel remineralization: Biomimetic apatite nanocrystals and fluoride ions different effects," J. Nanomater., vol. 2009, 2009, doi: 10.1155/2009/746383.

[8] S. C. Wu, Y. L. Kao, Y. C. Lu, H. C. Hsu, and W. F. Ho, "Preparation and characterization of microrod hydroxyapatite bundles obtained from oyster shells through microwave irradiation," J. Aust. Ceram. Soc., vol. 57, no. 5, pp. 1541–1551, Dec. 2021, doi: 10.1007/s41779-021-00657-3.

[9] A. Szcześ, L. Hołysz, and E. Chibowski, "Synthesis of hydroxyapatite for biomedical applications," Adv. Colloid Interface Sci., vol. 249, pp. 321–330, 2017, doi: 10.1016/j.cis.2017.04.007.

[10] P. Phatai, C. M. Futalan, S. Kamonwannasit, and P. Khemthong, "Structural characterization and antibacterial activity of hydroxyapatite synthesized via sol-gel method using glutinous rice as a template," J. Sol-Gel Sci. Technol., vol. 89, no. 3, pp. 764–775, 2019, doi: 10.1007/s10971-018-4910-9.

[11] M. Sadat-Shojai, M. T. Khorasani, E. Dinpanah-Khoshdargi, and A. Jamshidi, "Synthesis methods for nanosized hydroxyapatite with diverse structures," Acta Biomater., vol. 9, no. 8, pp. 7591–7621, 2013, doi: 10.1016/j.actbio.2013.04.012.

[12] M. A. M. Castro et al., "Synthesis of hydroxyapatite by hydrothermal and microwave irradiation methods from biogenic calcium source varying pH and synthesis time," Bol. la Soc. Esp. Ceram. y Vidr., vol. 61, no. 1, pp. 35–41, 2022, doi: 10.1016/j.bsecv.2020.06.003.

[13] J. Chen, J. Liu, H. Deng, S. Yao, and Y. Wang, "Regulatory synthesis and characterization of hydroxyapatite nanocrystals by a microwave-assisted hydrothermal method," Ceram. Int., vol. 46, no. 2, pp. 2185–2193, 2020, doi: 10.1016/j.ceramint.2019.09.203.

[14] Y. Guesmi, H. Agougui, R. Lafi, M. Jabli, and A. Hafiane, "Synthesis of hydroxyapatite-sodium alginate via a co-precipitation technique for efficient adsorption of Methylene Blue dye," J. Mol. Liq., vol. 249, pp. 912–920, 2018, doi: 10.1016/j.molliq.2017.11.113.

[15] MS Al-Ajely, KM Ziadan, RM Al-Bader -"Preparation and characterization of calcium fluoride nano particles for dental applications" Int J Res-Granthaalayah, 2018

[16] M. García-Guaderrama, O. Ceballos-Sanchez"N-doped TiO2 nanoparticles obtained by a facile coprecipitation method at low temperature" April 2018, Pages 5273-5283

[17] N. N. Panda, K. Pramanik, and L. B. Sukla, "Extraction and characterization of biocompatible hydroxyapatite from fresh water fish scales for tissue engineering scaffold," Bioprocess Biosyst. Eng., vol. 37, no. 3, pp. 433–440, 2014, doi: 10.1007/s00449-013-1009-0.

[18] R. Mustaffa, M. R. Mohd Yusof, and Y. Abdullah, "A Novelty of Synthetic Hydroxyapatite from Cockle Shell and Characterization," Adv. Mater. Res., vol. 1087, pp. 429–433, 2015, doi: 10.4028/www.scientific.net/amr.1087.429.

[19] S. Nayar and A. Guha, "Waste utilization for the controlled synthesis of nanosized hydroxyapatite," Mater. Sci. Eng. C, vol. 29, no. 4, pp. 1326–1329, 2009, doi: 10.1016/j.msec.2008.10.002.

[20] J. Klinkaewnarong and S. Utara, "Ultrasonic-assisted conversion of limestone into needle-like hydroxyapatite nanoparticles," Ultrason. Sonochem., vol. 46, pp. 18–25, 2018, doi: 10.1016/j.ultsonch.2018.04.002.

[21] S. Rujitanapanich, P. Kumpapan, and P. Wanjanoi, "Synthesis of hydroxyapatite from oyster shell via precipitation," in Energy Procedia, 2014, vol. 56, no. C, pp. 112–117, doi: 10.1016/j.egypro.2014.07.138.

[22] [22] M. Akram, R. Ahmed, I. Shakir, W. A. W. Ibrahim, and R. Hussain, "Extracting hydroxyapatite and its precursors from natural resources," J. Mater. Sci., vol. 49, no. 4, pp. 1461–1475, 2014, doi: 10.1007/s10853-013-7864-x.

[23] S. C. Wu, H. C. Hsu, S. K. Hsu, C. P. Tseng, and W. F. Ho, "Preparation and characterization of hydroxyapatite synthesized from oyster shell powders," Adv. Powder Technol., vol. 28, no. 4, pp. 1154–1158, 2017, doi: 10.1016/j.apt.2017.02.001.

[24] Meier,Crystallite size measurement using X-ray diffraction.Department of Chemical Engineering and Materials Science,University of California,Davis September,2004.13.

[25] K. Kuroda, R. Ichino, M. Okido, and O. Takai, "Effects of ion concentration and pH on hydroxyapatite deposition from aqueous solution onto titanium by the thermal substrate method," J. Biomed. Mater. Res., vol. 61, no. 3, pp. 354–359, 2002, doi: 10.1002/jbm.10197.

[26] M.S. Al-Ajely, K.M. Ziadan, R.M. Al-Bader, PREPARATION AND CHARACTERIZATION OF CALCIUM FLUORIDE NANO PARTICLES FOR DENTAL APPLICATION, Int J Res Granthaalayah, 6 (2018) 338-346

[27] P. Zhu, Y. Masuda, and K. Koumoto, "The effect of surface charge on hydroxyapatite nucleation," Biomaterials, vol. 25, no. 17, pp. 3915–3921, 2004, doi: 10.1016/j.biomaterials.2003.10.022.

[28] A. Shavandi, A. E. D. A. Bekhit, A. Ali, and Z. Sun, "Synthesis of nano-hydroxyapatite (nHA) from waste mussel shells using a rapid microwave method," Mater. Chem. Phys., vol. 149, pp. 607–616, Jan. 2015, doi: 10.1016/j.matchemphys.2014.11.016.

[29] A. Pal, S. Paul, A. R. Choudhury, V. K. Balla, M. Das, and A. Sinha, "Synthesis of hydroxyapatite from Lates calcarifer fish bone for biomedical applications," Mater. Lett., vol. 203, pp. 89–92, 2017, doi: 10.1016/j.matlet.2017.05.103.

[30] D. Haverty, S. A. M. Tofail, K. T. Stanton, and J. B. McMonagle, "Structure and stability of hydroxyapatite: Density functional calculation and Rietveld analysis," Phys. Rev. B - Condens. Matter Mater. Phys., vol. 71, no. 9, pp. 1–9, 2005, doi: 10.1103/PhysRevB.71.094103.

[31] D. Núñez, E. Elgueta, K. Varaprasad, and P. Oyarzún, "Hydroxyapatite nanocrystals synthesized from calcium rich bio-wastes," Mater. Lett., vol. 230, pp. 64–68, 2018, doi: 10.1016/j.matlet.2018.07.077.

[32] M. Sari and Y. Yusuf, "Synthesis and characterization of hydroxyapatite based on green mussel shells (perna viridis) with the variation of stirring time using the precipitation method," in IOP Conference Series: Materials Science and Engineering, Nov. 2018, vol. 432, no. 1, doi: 10.1088/1757-899X/432/1/012046.

[33] H. A. Permatasari and Y. Yusuf, "Characteristics of Carbonated Hydroxyapatite Based on Abalone Mussel Shells (Halioitis asinina) Synthesized by Precipitation Method with Aging Time Variations," in IOP Conference Series: Materials Science and Engineering, Jul. 2019, vol. 546, no. 4, doi: 10.1088/1757-899X/546/4/042031.

[34] Almukarrama and Y. Yusuf, "Development carbonated hydroxyapatite powders from oyster shells (Crassostrea gigas) by carbonate content variations," in Materials Science Forum, 2020, vol. 975 MSF, pp. 76–81, doi: 10.4028/www.scientific.net/MSF.975.76.

[35] "Physical-mechanical properties of dental composites by addition oyster shell powder as fillers ," Basrah Journal of Science. 2019.